Progress In Electromagnetics Research M, Vol. 83, 191–202, 2019

A Small Cost-Effective Super Ultra-Wideband Microstrip Antenna with Variable Band-Notch Filtering and Improved Radiation Pattern with 5G/IoT Applications

Hamid R. D. Oskouei[1, *], Amir R. Dastkhosh[2], Alireza Mirtaheri[3], and Mehdi Naseh[4]

Abstract—In this work, a new design of small microstrip antenna with variable band-notched filtering characteristic for super ultra-wideband (UWB) applications including 5G/IoT networks is presented. In the proposed structure by creating steps with optimized appropriate sizes and angles in the lower edges of the quasi-square patch antenna and by a new technique of modifying the ground plane, more efficient radiation patterns and characteristic impedance are achieved. Moreover, the omnidirectional low cross-polarized H-plane radiation patterns are obtained in frequency band of 3–11 GHz. Also, its radiation patterns are improved between 11 and 14.5 GHz and have better performance especially with tuning capacitors between 14.5 and 20 GHz. In addition, its frequency bandwidth with VSWR < 2 is from 3 GHz to 50 GHz which covers 5G networks and both ultra-wideband (UWB) and super wideband (SWB) communications. A rectangular slot on the patch is used to create an integrated band-notch filter in the structure to avoid interference with other wireless systems like wireless local area networks (WLANs), and this specification can be activated or deactivated by a PIN diode. In addition, the center frequency of the filter can be tuned by just a varactor diode or a variable capacitor and/or by changing the position of the capacitors in frequency range of about 3.5–6 GHz, which rejects interference of all WLANs and even their lower and upper bands, and nulls in the radiation patterns can be changed especially in upper bands as well. The final structure simulation results are in good agreement with measurement ones.

1. INTRODUCTION

The mobile communication will progress and develop more and more, with wireless data traffic projected to increase 10,000 fold within the next 20 years, due to increased usage of smartphones, tablets, new wireless devices, and the Internet of Things (IoT). To meet this ever increasing demand in capacity and to support 5G (5th Generation Networks) requirements greater than 10 Gbps peak and edge rates greater than 100 Mbps for extreme mobile broadband (eMBB) applications, one has to use a new spectrum beyond sub-6 GHz frequencies. Due to the availability of large bandwidths at mmWave frequencies, the 5G requirements for eMBB can be met using a simple air interface and high dimension phased arrays. mmWave systems also face inherent challenges, such as high penetration loss, higher sensitivity to blockage, and diminished diffraction, which the system must overcome. The higher frequencies used for 5G enable higher data transmission through wider channels and cause reducing latency significantly compared to current levels. In 2002, Federal Communications Commission (FCC) assigned frequency band 3.1–10.6 GHz for ultra-wideband (UWB) systems [1]. Some UWB systems and their applications have been introduced in references like [2–7].

Received 18 May 2019, Accepted 19 July 2019, Scheduled 14 August 2019
* Corresponding author: Hamid R. D. Oskouei (h.b.s.dalili@gmail.com).
[1] Shahid Sattari Aeronautical University of Science & Technology, Tehran, Iran. [2] Amir Reza Dastkhosh, Sahand University of Technology, Iran. [3] Shahid Sattari Aeronautical University of Science & Technology, Tehran, Iran. [4] University of Bologna, Italy.

Also, on July 14, 2016, the US Federal Communications Commission (FCC) adopted new rules for wireless broadband operations above 24 GHz, making the U.S. the first country to make this spectrum available for next generation wireless services. The FCC allocated approximately 11 GHz for flexible, mobile, and fixed use of wireless broadband, comprising 7 GHz of unlicensed spectrum from 64 to 71 GHz and 3.85 GHz of licensed spectrum, designated as a new "upper microwave flexible use" service, in three bands: 27.5 to 28.35 GHz, 37 to 38.6 GHz, and 38.6 to 40 GHz. Table 1 illustrates the breakdown of the major frequencies established for use in 5G networks. FR1 will likely be used for initial implementations, with FR2 following. The second chart lists the FR2 frequency bands of interest. The FCC has also opened up spectrum from 64 GHz to 71 GHz for future activity [6–9]. As we know, wireless sensor networks like zigbee, LDWA, LoRa, WWAN, and mobile radio networks comprising 2G, 3G, 4G, and coming 5G need wider frequency bandwidth, data processing, and machine learning for optimum performance. Also, there are numerous applications and demands for faster wireless networks like less response time (40 times faster).

Table 1. Proposed 5G frequencies in details.

Band	Frequency (MHz)	Type
FR1	450–6000	Sub-6 GHz
FR2	24250–52600	mm-Wave

5G NR Band	Band Alias (GHz)	Uplink Band (GHz)	Downlink Band (GHz)	Bandwidth (GHz)	Type
n257	28	26.5–29.5	26.5–29.5	3	TDD
n258	26	24.25–27.5	24.25–27.5	3.25	TDD
n260	39	37–40	37–40	3	TDD

Among different kinds of antennas, as one of main parts of any communication system, printed monopole antennas are more considered in UWB applications since they fulfill all required parameters. Although a large number of UWB antennas have been designed with a compact size in recent years [9–14], their upper frequencies are less than 10.6 GHz. Moreover, their omnidirectional H-plane radiation patterns are limited to about 3 to 10 GHz. For example, in [12] a novel super-wideband (SWB) antenna with an optimized feed is presented, and its bandwidth is from 1.05 to 32.7 GHz with VSWR < 2, whereas the size of antenna is partly large, and H-plane radiation pattern of the antenna in the frequency range not only is not omnidirectional but also has high cross polarization.

On the other hand, there are many narrowband wireless communication systems in the UWB spectrum such as WLANs (5.15–5.825) which can cause interferences with other communication systems especially UWB ones due to their stronger power density. So, UWB systems have to be capable of interference rejection, and a conventional solution is adding a filter to the system. However, designing a filter increases dimensions of the system, is costly, and needs modern optimization techniques. Consequently, the designers have to try different design methods which are time-consuming [13, 14]. In this paper according to Fig. 1, for overcoming interference problem, a slot in the radiation patch is designed and used. Some methods have been investigated and applied in references [15–17]. These techniques include etching shaped slots in the feed line or radiation patch [18, 19], using rectangular split-ring resonators [20], using parasitic components [7], etc. Nonetheless, in SWB systems such as [12], using band-rejection is overlooked. In a square monopole antenna like [11], horizontal surface currents (relative to the x axis) flow in the lower edge of the radiation patch and are bigger than the vertical ones which can reduce the bandwidth and degrade the radiation performance at higher frequencies (specially > 10 GHz). In this paper by modifying and optimizing the structure of the antenna, a balance between the components of vertical and horizontal surface currents on the patch is created for better performance. In other words, improved radiation patterns have been obtained in super UWB (SUWB) frequency range by modifying patch, ground plane, and feed line. By carving aperture slots

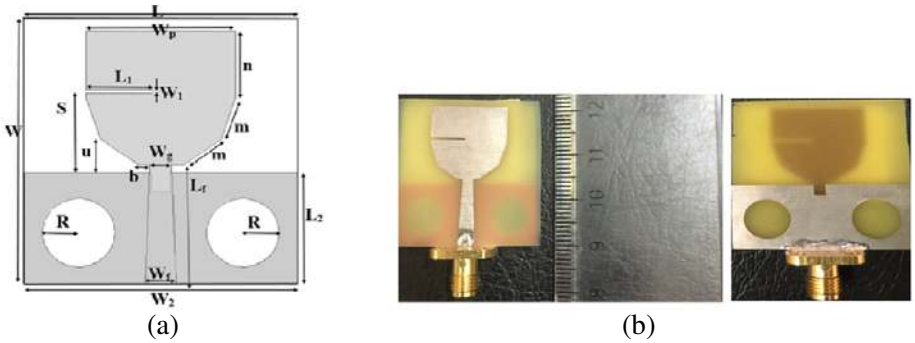

Figure 1. Geometry of the proposed antenna; (a) View of the proposed antenna. (b) Top/bottom prototype of the proposed antenna.

on the ground plane, the unwanted current distributions decrease, and better radiation patterns are achieved up to 14 GHz. Finally, the proposed optimized antenna is simulated by Ansys HFSS software on FR4 and also Rogers TMM4 substrates and is fabricated and measured. The bandwidth of the proposed antenna is from 3 to 50 GHz. Radiation patterns are omnidirectional from 3 to 11 GHz, and better radiation pattern performance can be achieved between 11 and 14 GHz with tuning capacitors and up to 20 GHz with optimization and adjustment (for example with a 2 pF tuning capacitor in 15 GHz). Moreover, center frequency of the band-notched filter can be tuned from 3.5 to 6 GHz by changing structure geometry and/or variable capacitor.

2. ANTENNA CONFIGURATION AND DESIGN

Figure 1 illustrates the geometry of the proposed antenna. The antenna is designed, simulated, and built on an FR-4 substrate with dimensions of 30 mm × 30 mm with permittivity (ε_r) of 4.4 and thickness (h) = 1.6 mm. In spite of that, for better comparison to low loss dielectric substrates, the antenna is simulated on a Rogers TMM4 substrate as well. In this section, design process and characteristics of the antenna are described completely. The antenna dimensions are (in millimeter): $W = 30$, $L = 30$, $W_2 = 30$, $L_2 = 13$, $W_1 = 0.4$, $W_f = 3.4$, $L_f = 13.95$, $W_g = 2.4$, $R = 4$, $S = 9.3$, $u = 3.93$, $b = 1.33$, $n = 7.79$, $m = 5.07$, $W_P = 16.4$, $L_1 = 7.3$).

2.1. Antenna Design and Matching

The design and improvement process and VSWR results of the proposed antennas are illustrated in Fig. 2 and Fig. 3, respectively. The primary antenna, shown in Fig. 2(a), has a square-like patch with a straight feed line and defected ground plane. In order to have better impedance matching and radiation performance, a small slot (2 mm × 2.2 mm) is placed on the ground plane. Because the structure of the antenna is similar to a disc microstrip one, the lowest frequency of the antenna can be calculated approximately from Equation (1) [17]:

$$fL = 7.2/((l + r + p) \times k)\,\text{GHz} \tag{1}$$

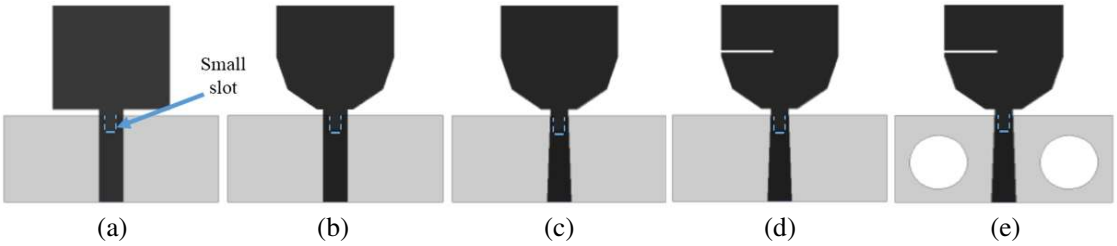

Figure 2. Proposed antenna designing process.

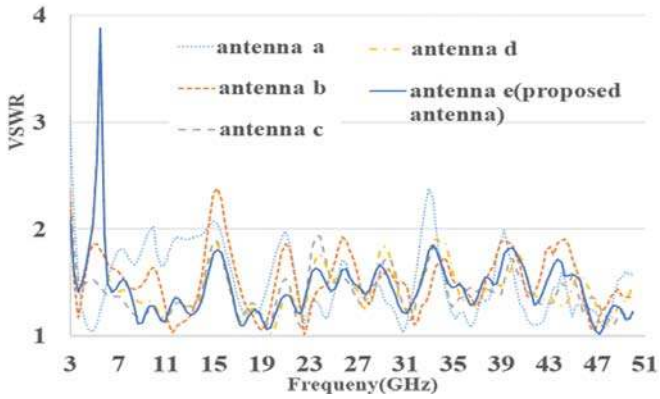

Figure 3. Simulated results of VSWR for the antenna models.

which can be a good estimate for the primary design. In Equation (1), $k = 1.15$, l is the height of the patch, p the air gap between the patch and ground plane, and r the effective radius of an equivalent cylindrical monopole antenna. As shown in Fig. 3, bandwidth of the primary antenna (antenna a) is from 3.4 to 10 GHz with VSWR < 2. Using a rectangular slot in the bottom edge of the patch is a method to create balance between the components of horizontal and vertical currents [21].

In this work as shown in Fig. 2, trapezoidal and triangular pieces are combined in the edges of the patch to create the antenna structure. As a result, the bandwidth of the second structure of Fig. 1 (antenna b) is increased to 11 GHz. As can be seen, we have reduction in the value of VSWR (Fig. 3). In the third structure (antenna c), a tapered feed line is replaced by the rectangle one. In the latter structure, a good impedance matching can be achieved for the entire bandwidth (3 to 50 GHz). Furthermore, the forth structure (antenna d) is developed by engraving a rectangular slot on the patch to eliminate a typical narrowband WLAN signal. Finally, the fifth structure (antenna e) is designed by creating two circular apertures on the ground plane to improve radiation performance and VSWR. A better description and details of the final antennas (d and e) have been expanded in Subsections 2.2 and 2.3.

2.2. Band-Notched Characteristics of the Antenna

In this section, various effects of dimensions of the rectangular slot using (variable) capacitors are investigated. In addition, the design of a band-notch filter for the antenna structure is explained. The band-notched property has harmful effects on the bandwidth. For example in [11], the VSWR of the proposed antenna without band-notched filter is nearly from 2.4 to 12.5 GHz, whereas using band-notched filter decreases the bandwidth to 2.4–11.2 GHz. In this reference, the antenna has ultra-wideband, and placing and/or adjusting band-notched filter does not decrease frequency bandwidth. Therefore, dimensions and location of the rectangular slot of the band-notched filter should be determined and selected correctly to have positive effect in the entire frequency range of the Super SUWB antenna.

As mentioned, frequency ranges of WLAN systems are from 4.85 to 5.83 GHz. Also, the center frequency of the band-notched antenna (fnotch) is defined by Equation (2), where c is the speed of light in free space, εr the dielectric constant, and $L1$ the length of the rectangular slot. $L1$ is nearly a quarter wavelength at the center frequency of the band-notched structure and can be calculated by [17]:

$$L2 = c/(2 \times fnotch \times \sqrt{((\varepsilon r + 1)/2)}) \tag{2}$$

Selected substrate for simulation and fabrication is FR4. Fig. 4 depicts VSWR results of the final simulated antenna with variations of dimensions of the rectangular slot ($L1$, $W1$, and S). As can be seen in Fig. 4(a), by varying $L1$ ($W1 = 0.4$ mm, $S = 9.3$ mm), the bandwidth and center frequency of the band-notched characteristic can be changed. Furthermore, Fig. 4(b) reveals that $W1$ ($L1 = 7.3$ mm, $S = 9.3$ mm) and S ($L_1 = 7.3$ mm, $W_1 = 0.4$ mm) determine the lowest and highest frequencies of the band-notched filter, respectively. In another configuration, a varactor diode or variable capacitor and/or

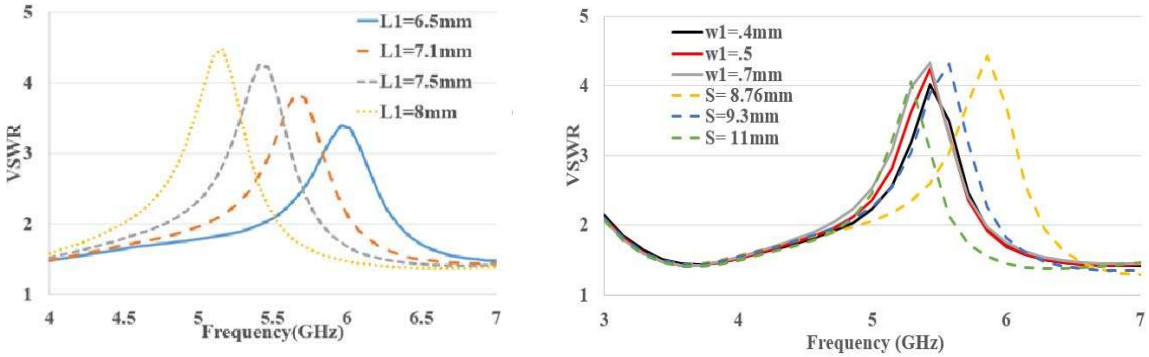

(a) (b)

Figure 4. Effects of slot parameters varying ($L1$, $W1$, and S) on FR4 substrate.

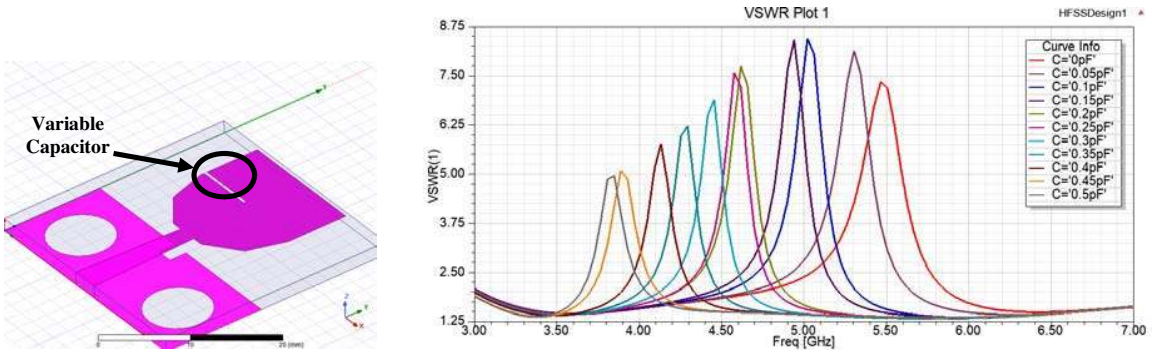

(a) (b)

Figure 5. Effects of adding and changing variable capacitor to the antenna; (a) antenna structure, (b) simulated results on Rogers TMM 4 substrate.

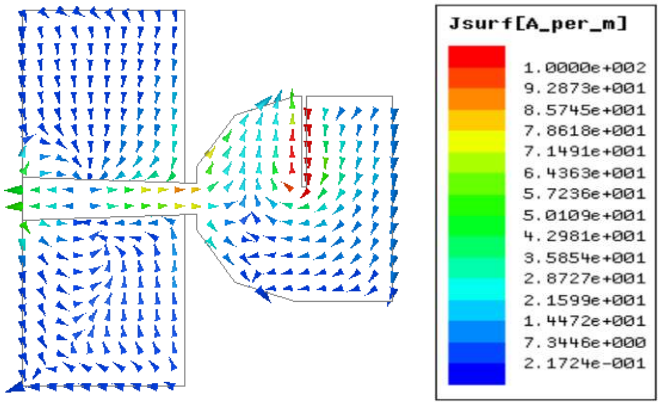

Figure 6. Simulated current distributions at 5.49 GHz.

capacitive slots are added in gap of the patch antenna, and the capacitor value is changed from 0 to 2 pF. The results are shown in Fig. 5 and illustrate that by using a variable capacitor, the center frequency of the band-notch filter of the antenna can be easily tuned.

The final dimensions of the rectangular slot band-notched filter are: $L1 = 7.3$ mm, $W1 = 0.4$ mm, and $S = 9.3$ mm. Fig. 6 shows the surface current distribution at fnotch = 5.49 GHz of the band-notched filter. As can be seen, the current distribution at 5.49 GHz is mainly near the rectangular

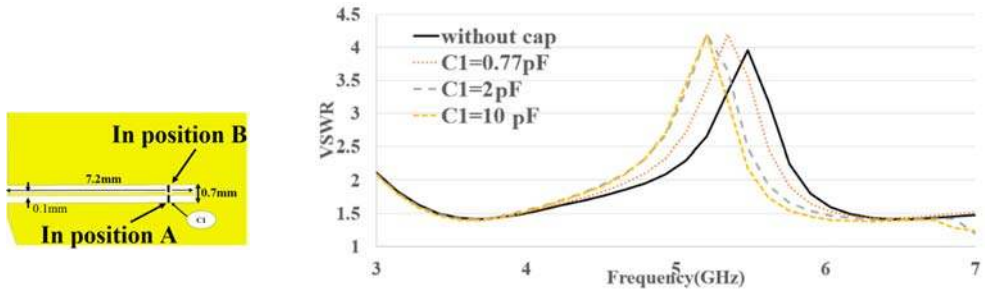

(a) (b)

Figure 7. (a) Capacitor and microstrip line added to the rectangular slot; (b) Measured VSWR for different values of $C1$.

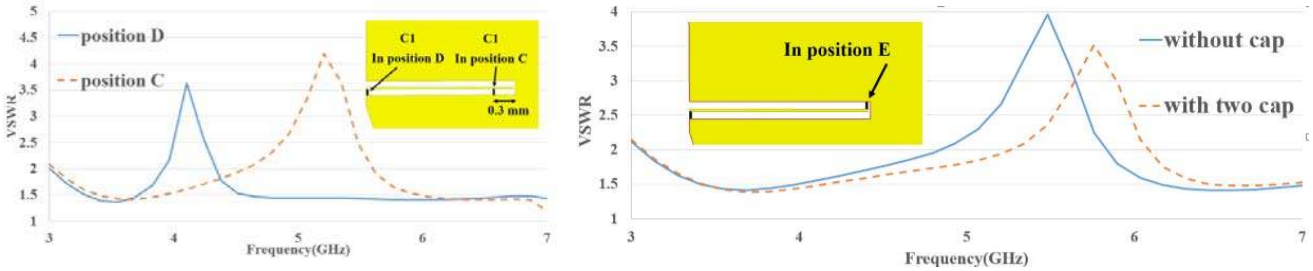

(a) (b)

Figure 8. (a) Measured VSWR for position C, D ($C1 = 2$ pF), (b) Measured VSWR with two capacitors and a microstrip line.

slot, and it cancels the excited surface currents close to the center frequency of the band-notched filter. Additionally, if a PIN diode switch is placed in the rectangular slot of the proposed antenna, the band-notched filter is switched on and off. When the switch is off, the antenna does not have any band-notched feature, and when it is on, the antenna becomes a super UWB antenna with variable frequency band-notched functioning. In another configuration and to change band-notched filter of the structure, a microstrip line or capacitive slot is inserted in the rectangular slot, then a capacitor (C1) is placed in position A, as depicted in Fig. 7(a). Then, the value of the capacitor is changed, and as disclosed in Fig. 7(b), the center frequency of the band-notched filter is changed. If the capacitor is inserted in position B, the ability of this capacitor for tuning center frequency of the band-notched filter is similar to the capacitor of position A. In addition, as shown in Fig. 8(a), by changing the capacitor position (2 pF for position C and D), the center frequency of the band-notched filter of the structure changes. As investigated in references [22–27], if another capacitor is added and placed in position E, frequency tuning specifications of the band-notched filter of the structure will be improved and cover higher and wider frequency ranges (Fig. 8(b)). In this case, the values of capacitors and the bigger distances between the capacitors are effective for more frequency tuning range which is nearly between 3.5 and 6.087 GHz.

For more and better frequency tuning range, other microstrip lines and capacitors can be added. In this case, each capacitor has its own frequency tuning effect. For instance, C1 is dominant for tuning, and C2 and Ci(s) are more suitable for better adjusting. Also, comparisons between the proposed antenna and other antennas in references with different aspects are illustrated in Table 2. The proposed antenna has a great bandwidth tuning capability, better performance, and small size. Also, better and more stable H-plane radiation patterns in frequency range between 3 GHz and 15 GHz with tuning capability and adjustments are achieved (for example with a 2 pF tuning capacitor or varactor diode in 15 GHz as mentioned before). Although the gap may not be wide enough for inserting an SMD capacitor or a diode, by using another structure (Fig. 5(a)) or die technology this issue can be solved. Simulated H-plane and E-plane radiation patterns in frequency range of 3–14 GHz are presented in Fig. 9. It

Table 2. Comparison between the proposed antenna and many antenna.

Ref	Size (mm^3)	Bandwidth	Planar	Device used	ε_r	Band-notched filter center frequency (GHz)	Tunable	Pattern Stability (GHz)
[**27**]	$80 \times 80 \times 20$	UWB	No	Capacitor	2.33	4.8–7.4	no	Up to 10
[**28**]	$100 \times 100 \times 19$	UWB	No	Diode	3.2	4.5–6.1	no	Up to 8
[**29**]	$77 \times 80 \times 0.76$	UWB	Yes	Diode	3.5	5.2–6.1	no	Up to 5.72
[**30**]	$30 \times 30 \times 0.8$	3.1–18	Yes	Diode	4.4	2.7–7.1	no	Up to 10
The proposed antenna	$30 \times 30 \times 1.6$	3–50 simulation	Yes	Capacitor/ Diode	4.4	3.5–6.087	Yes	Up to 14
		3–40 measurement		Capacitor/ Diode				

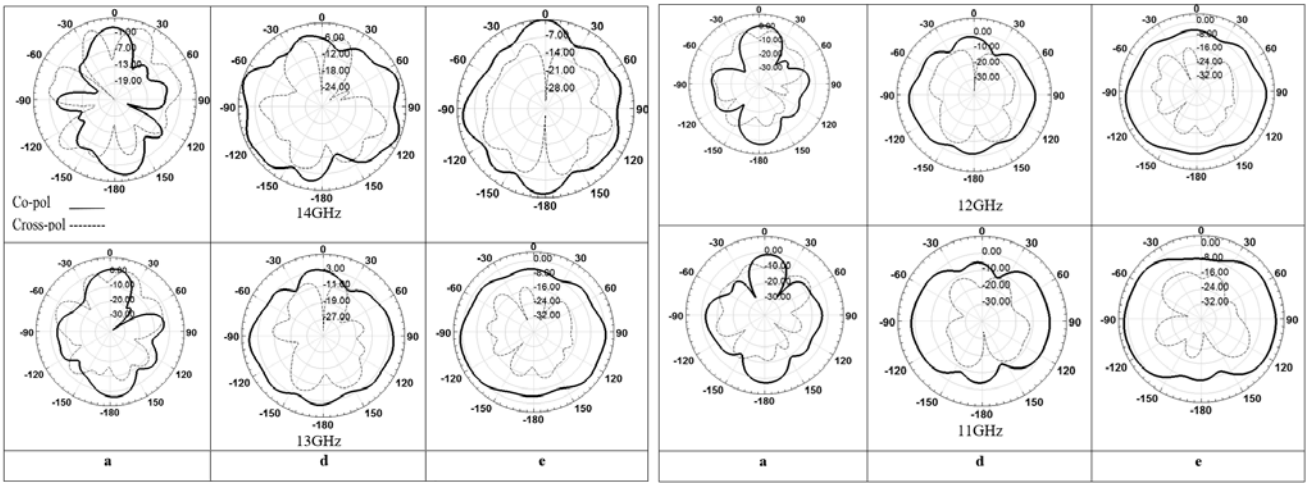

Figure 9. Simulated H-plane radiation patterns of antennas a, d and e at 4 different frequencies.

delineates that H-plane patterns are improved, and E-plane patterns are bidirectional. As shown in Figs. 9 and 13, stable and better H-plane radiation patterns up to 20 GHz (with adjustment of tuning capacitors and/or optimization) are obtained. At higher frequencies of 14 GHz, the cross-polarization level rises due to the increase of orthogonal surface currents.

2.3. Radiation Patterns

Due to the coupling effects between the patch and ground plane, the ground plane geometry has an important role in UWB antenna performance. Most articles only use defected ground structures (DGSs) and create slots in the ground plane to improve bandwidth such as [18] and [24]. Nevertheless, a few articles consider and investigate effects of the ground planes. It has been proved that radiation patterns are dependent to dimensions and shapes of the ground plane [25–35]. Moreover, in references, radiation patterns are only improved in frequency range of 3–10 GHz. For example in [25], a UWB antenna with two ground planes ($32 \times 15\,mm^2$ and $70 \times 15\,mm^2$) is used, and L-shaped slots are carved on the top edges of ground planes. The radiation patterns of the antenna with large ground planes, with and without slots, are very similar. The only differences are at lower frequencies whereas the cross-polarized electromagnetic fields are smaller for the antenna with slots in the ground plane. Anyhow, radiation patterns of the antennas are improved for UWB applications. Nonetheless, two problems are

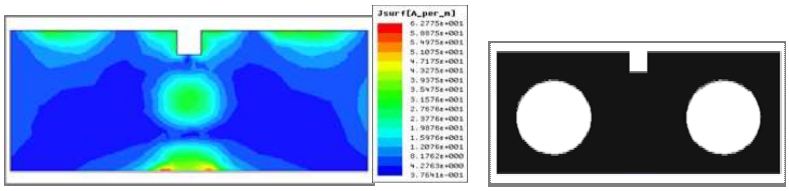

(a) (b)

Figure 10. (a) Simulated current distributions for SWB antenna at 12 GHz. (b) Geometry of the modified ground of SWB antenna.

not investigated: firstly, radiation patterns of the antenna with small ground planes (32 mm × 15 mm with slot) and secondly, the reasons for selecting positions of the slots in ground planes.

In this part, radiation patterns and gain of the proposed antenna are illustrated in the following figures. The simulated H-plane radiation patterns of antennas (a), (d), and (e) at 4 different frequencies are shown in Fig. 9. As can be seen, H-plane radiation patterns of antenna (d) are significantly improved by modifying the patch and feed line. In addition, the simulation of the surface current distribution for the ground plane of antenna (d) at 12 GHz is shown in Fig. 10(a). In some places, amplitudes of surface currents have the minimum values compared to other places. So, for improving radiation properties, according to the minimum current amplitudes, two circular apertures with the radius of $R = 4$ mm are subtracted from the ground plane (Figs. 1 and 10(b)). Fig. 9 shows that by subtracting two circular apertures from the ground plane, H-plane radiation pattern of antenna (e) is more omnidirectional and in wider frequency range than antenna (d). Also, bandwidth of the modified antenna is much wider than that mentioned and other antennas in references [3–9]. Furthermore, the antenna has a variable band-notched filtering feature.

In summary, an antenna with wider frequency bandwidth, radiation pattern, and variable band-notched filtering characteristic has been achieved, and H-plane radiation has also been improved up to 14 GHz by carving aperture slots on the ground plane. In addition, at higher frequencies the cross-polarized electromagnetic fields rise due to the increasing orthogonal surface currents.

3. MEASUREMENT AND SIMULATION RESULTS

The fabricated antenna is shown in Fig. 1(b), and the results of simulation and measurement of the proposed antenna are shown in Figs. 11–15. As can be seen, there is a significant agreement between the results of simulations and measurements, and the small differences are due to the effects of fabrication process and SMA connector. The return loss of the proposed antenna is measured by Agilent E8363C PNA network analyzer. Fig. 12(a) shows the gain of antenna (e). The antenna has been simulated in frequency range of 3–40 GHz, because the measured VSWR is up to 40 GHz. As can be seen, the gain

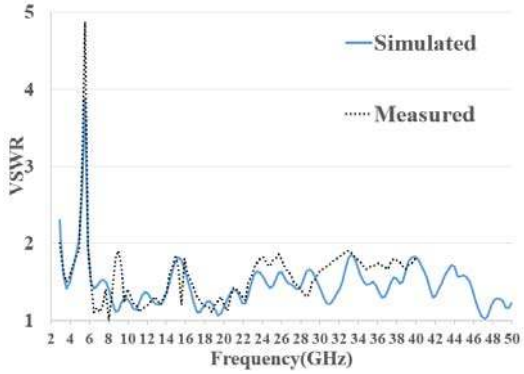

Figure 11. Simulated and measured VSWR of the proposed antenna.

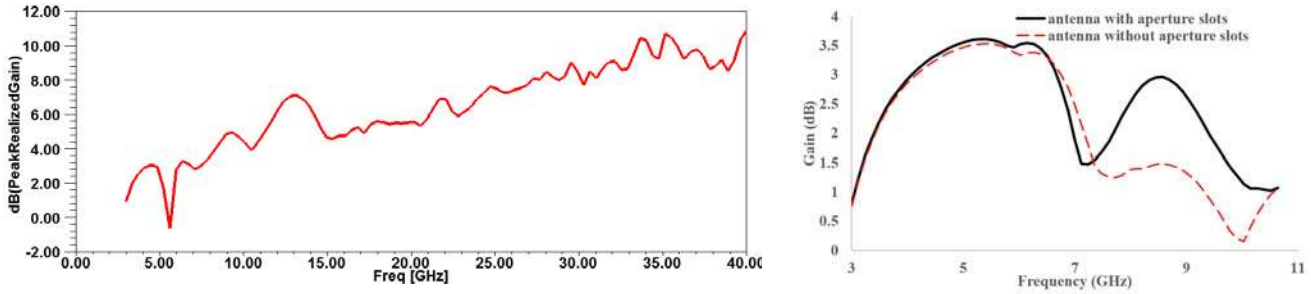

(a) (b)

Figure 12. (a) Simulated peak gain of the SWB antenna with band-notched. (b) Gain of the proposed antenna without band-notched (with aperture slots and without aperture slots).

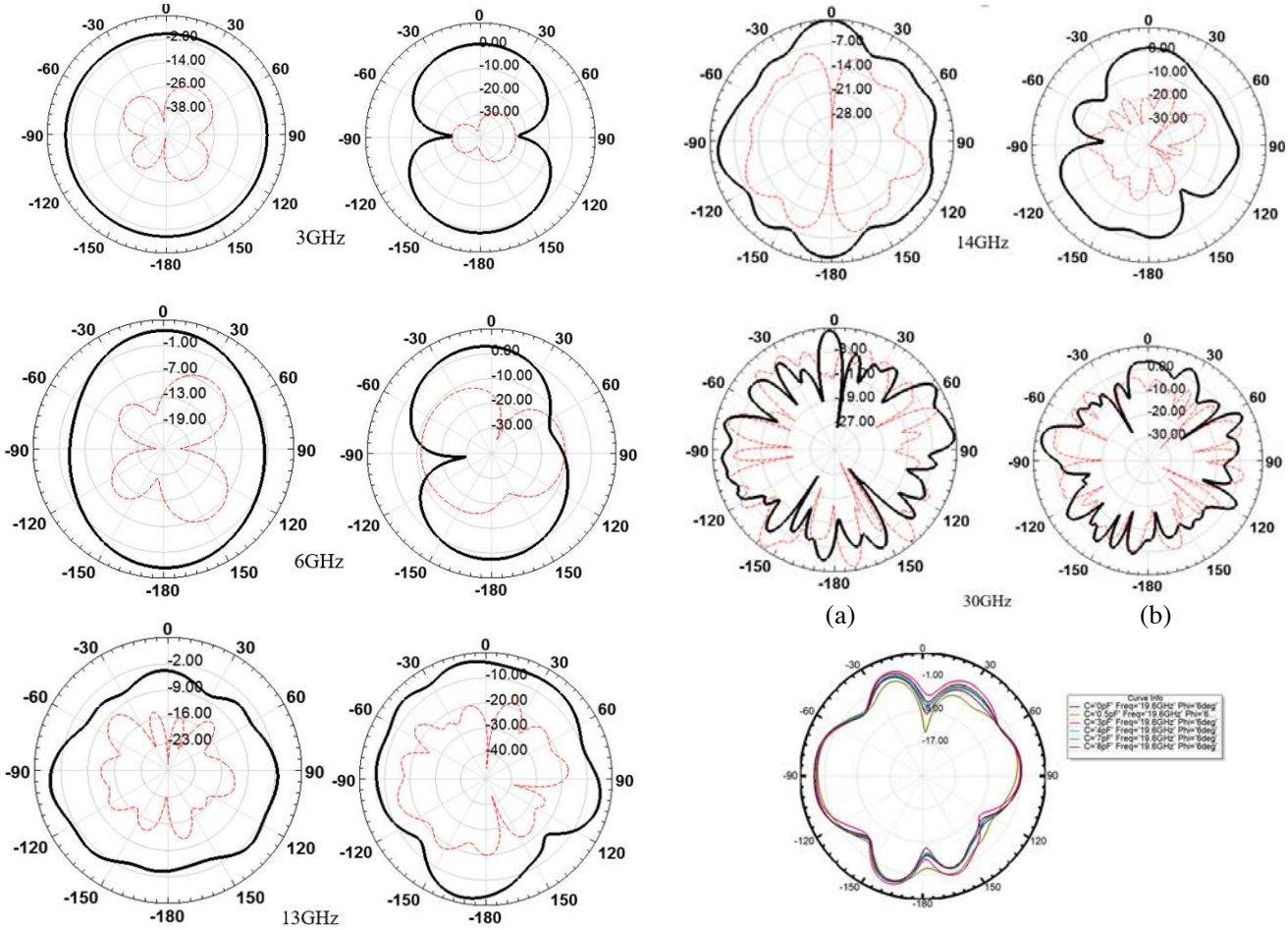

(a) (b) (a) (b) (a) (b) (c)

Figure 13. Radiation patterns for antenna; e (solid line: co-pol; dashed line: cross-pol), (a) measured H-plane radiation patterns, (b) measured E-plane radiation patterns, (c) simulated H-plane radiation pattern of the antenna as a function of one tuning capacitor at 19.6 GHz.

of the proposed antenna drops at WLAN band (−2.4 dB at 5.49 GHz), and minimum gain is 1 dB in 3 GHz and maximum gain 9.47 dB in 31.3 GHz. In addition, the gain of the proposed antenna without the band-notched filter structure is presented in Fig. 12(b) (with aperture slots and without aperture slots), and it shows that the gain of the antenna with aperture slots is better than the antenna without

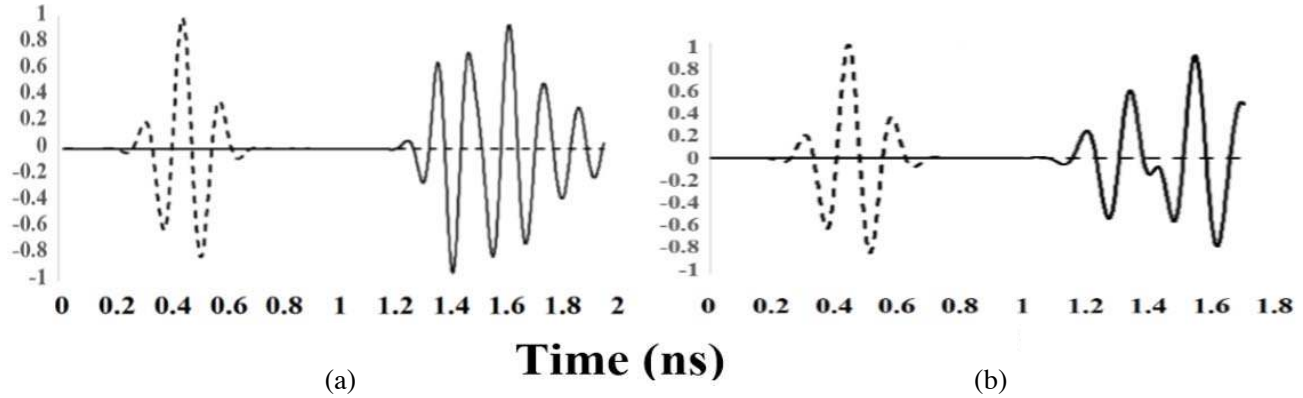

Figure 14. Received and transmitted pulse for the antenna (a) face to face (b) side by side.

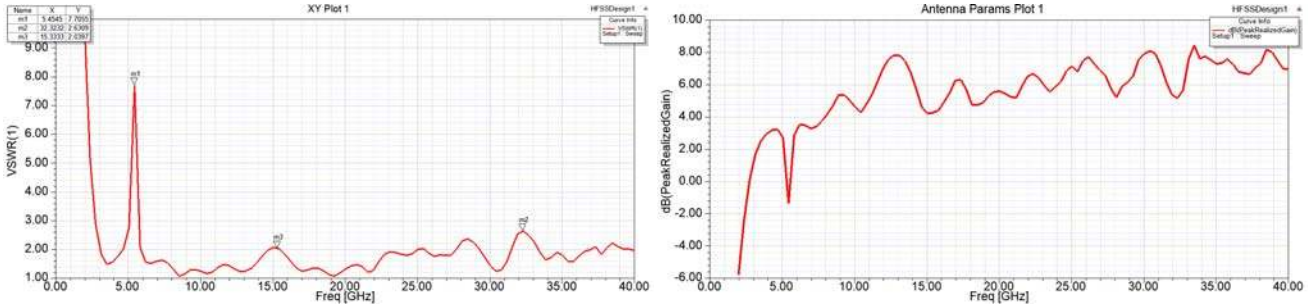

Figure 15. (a) Simulated VSWR, and (b) Simulated peak gain of the SWB antenna with band-notched on low-loss dielectric substrate (Rogers TMM 4 with dielectric loss tangent = 0.002).

them.

Furthermore, measured radiation patterns of the final SUWB antenna in the H-plane and E-plane at 3, 6, 14, 30 GHz are shown in Figs. 13(a) and (b), respectively. Fig. 13 also illustrates that at frequencies less than 14 GHz, the radiation patterns of the antenna are improved and bidirectional. Also, at higher frequencies (for example 30 GHz), the cross-polarized electromagnetic fields increase due to more orthogonal surface currents. Additionally, H-plane radiation pattern of the antenna as a function of one tuning capacitor value at 19.6 GHz is depicted in Fig. 13(c) which shows that with varying capacitor value, nulls in radiation pattern can be changed. In addition, time domain characteristic of the antenna without band-notched filter is analyzed by CST Microwave Studio. For this simulation, antennas are placed in the far field region (face to face and side by side), and the transmitter antenna is excited by a Gaussian signal (3–11 GHz). The received and transmitted signals are shown in Fig. 14. According to this figure, the antenna has improved performance in time domain. Fidelity factors of face to face and side by side configurations are 0.81 and 0.72, respectively.

Finally, for better comparison and investigation of the antenna performance in low-loss dielectric substrates, the structure is simulated on Rogers TMM 4 with loss tangent of 0.002 too, and the same results are obtained. The results are illustrated in Fig. 15.

4. CONCLUSION

A compact super ultra-wideband antenna with variable band-notched filtering characteristic has been presented. The modified structure of the patch, with its 50-Ω tapered feed line and engraving slots on the ground plane, provides a wider impedance bandwidth (3 to 50 GHz) and lower cross polarized and omnidirectional radiation patterns than similar antennas in the literature. This antenna can be used in

a very wide frequency range including 5G network. The WLAN band is filtered by a quarter wave slot and capacitors, and the center frequency of the rejection filter can be tuned by using constant and/or variable capacitors in the patch. Some nulls in the radiation patterns can be changed by utilizing this technique. Small size, ideal return loss in total frequency range, and improved radiation patterns of the proposed antenna make it an appropriate candidate for UWB and SWB applications. Although this antenna has a simple and cost-effective structure, it is very versatile and efficient especially in comparison with intricate antennas.

REFERENCES

1. First Report and Order in the matter of Revision of Part 15 of the Commission's Rules Regarding Ultra-Wideband Transmission Systems, Released by Federal Communications Commission, ET-Docket 98-153, 2002.
2. Liu, L.-L., et al., "A compact band-notch ultra-wideband antenna," *2017 International Workshop on Electromagnetics: Applications and Student Innovation Competition (iWEM)*, IEEE, 2017.
3. Ali, J., et al., "Ultra-wideband antenna design for GPR applications: A review," *International Journal of Advanced Computer Science and Applications*, Vol. 8, No. 7, 392–400, 2017.
4. Awais, Q., et al., "A novel dual ultrawideband CPW-fed printed antenna for internet of things (IoT) applications," *Wireless Communications and Mobile Computing*, Vol. 2018, 2018.
5. Cicchetti, R., E. Miozzi, and O. Testa, "Wideband and UWB antennas for wireless applications: A comprehensive review," *International Journal of Antennas and Propagation*, Vol. 2017, 2017.
6. Ahmed, F., N. Hasan, and M. H. M. Chowdhury, "A compact low-profile ultra wideband antenna for biomedical applications," *International Conference on Electrical, Computer and Communication Engineering (ECCE)*, IEEE, 2017.
7. Franchina, V., et al., "A UWB antenna for X-band automotive applications," *2016 IEEE International Symposium on Antennas and Propagation (APSURSI)*, IEEE, 2016.
8. Kundu, S. and S. K. Jana, "Leaf-shaped CPW-fed UWB antenna with triple notch bands for ground penetrating radar applications," *Microwave and Optical Technology Letters*, Vol. 60, No. 4, 930–936, 2018.
9. *Microwave Journal*, Vol. 62, No. 3, Mar. 2019.
10. Kazim, J., A. Bibi, M. Rauf, M. Tariq, and O. Owais, "A compact planner dual-band-notched monopole antenna for UWB application," *Microw. Opt. Tecnol. Lett.*, Vol. 56, No. 5, 1095–1097, Mar. 2014, doi: 10.1002/mop.28270.
11. Liu, H.-W., C.-H. Ku, T.-S. Wang, and C.-F. Yang, "Compact monopole antenna with band-notched characteristic for UWB application," *IEEE Antennas. Wirel. Propag. Lett.*, Vol. 9, 397–400, May 2010, doi: 10.1109/LAWP.2010.2049633.
12. Liu, J., K. P. Esselle, S. G. Hay, and S. S. Zhong, "Compact super wide band asymmetric monopole antenna with dual-branch feed for bandwidth enhancement," *Electron. Lett.*, Vol. 49, No. 8, 2013.
13. Singh, U. and R. Salgotra, "Synthesis of linear antenna array using flower pollination algorithm," *Neural Computing and Applications*, Vol. 29, No. 2, 435–445, 2018.
14. Gevorkyan, A. V., T. Yu Privalova, and Yu V. Yukhanov, "Radiation characteristics of the low profile dipole antenna," *2018 Progress In Electromagnetics Research Symposium (PIERS — Toyama)*, 1621–1625, Japan, Aug. 1–4, 2018.
15. Li, W. T., X. W. Shi, and Y. Q. Hey, "Novel planar UWB monopole antenna with triple band-notched characteristics," *IEEE Antennas. Wirel. Propag. Lett.*, Vol. 8, 1094–1098, Oct. 2009, doi: 10.1109/LAWP.2009.2033449J.
16. Ray, K. P. and Y. Ranga, "Ultra wideband printed elliptical monopole antennas," *IEEE Trans. Antennas Propag.*, Vol. 55, No. 4, 1189–1192, 2007.
17. Gao, P., L. Xiong, J. Dai, S. He, and Y. Zheng, " Compact printed wide-slot UWB antenna with 3.5/5.5-GHz dual band-notched characteristics," *IEEE Antennas. Wirel. Propag. Lett.*, Vol. 12, 983–986, 2013.

18. Choukiker, Y. K. and S. K. Behera, "Modified Sierpinski square fractal antenna covering ultra-wide band application with band notch characteristics," *IET Microw. Antennas Propag.*, Vol. 8, No. 7, 506–512, May 2014, doi: 10.1049/iet-map.2013.0235.
19. Kelly, J. R., P. S. Hall, P. Jardner, and F. Ghanem, "Integrated narrow/band-notched UWB antenna," *Electron. Lett.*, Vol. 46, No. 12, 814–816, Jun. 2010, doi: 10.1049/el.2010.3368.
20. Sarkare, D., K. V. Srivastava, and K. Saurav, "A compact microstrip-fed triple band-Notched," *IEEE Antennas. Wirel. Propag. Lett.*, Vol. 13, 396–399, Feb. 2014, doi: 10.1109/LAWP.2014.2306812.
21. Jung, J., W. Choi, and J. Choi, "A small wideband microstrip-fed monopole antenna," *IEEE Microw. Wireless Compon. Lett.*, Vol. 15, No. 10, 703–705, Oct. 2005.
22. Heon, D. H., H. Y. Yang, and Y. K. Cho, "Tapered slot antenna with band-notched function for ultrawideband radios," *IEEE Antennas. Wirel. Propag. Lett.*, Vol. 11, 682–685, 2012.
23. Tripathi1, S., A. Mohan, and S. Yadav, "Hexagonal fractal ultra wideband antenna using Koch geometry with bandwidth enhancement," *IET Microw. Antennas Propag.*, Vol. 8, No. 15, 1445–1450, 2014.
24. Fereidoony, F., S. Chamaani, and A. Mirtaheri, "Systematic design of UWB monopole antennas with stable omnidirectional radiation pattern," *IEEE Antennas. Wirel. Propag. Lett.*, Vol. 11, 752–755, 2012.
25. Lu, Y., Y. Huang, H. T. Chattha, and P. Cao, "Reducing ground-plane effects on UWB monopole antennas," *IEEE Antennas Wireless Propag. Lett.*, Vol. 10, 147–150, 2011.
26. Ammann, M. J. and M. John, "Optimum design of the printed strip monopole," *IEEE Antennas and Propagation Magazine*, Vol. 47, No. 6, Dec. 2005.
27. Hu, Z. H., P. S. Hall, J. R. Kelly, and P. Gardner, "UWB pyramidal monopole antenna with wide tunable band-notched behavior," *Electron. Lett.*, Vol. 46, No. 24, 1588–1590, 2010.
28. Antonino-Daviu, E., M. Cabedo-Fabres, M. Ferrando-Bataller, and A. V. Jamenez, "Active UWB antenna with tunable band-notched behavior," *Electron. Lett.*, Vol. 43, No. 18, 959–960, 2007.
29. Jeong, W.-S., D.-Z. Kim, W.-G. Lim, and J. W. Yu, "Tunable bandnotch ultra wideband planar monopole antenna using varactor," *Microw Opt. Technol. Lett.*, Vol. 51, No. 12, 2829–2832, 2009.
30. Aghdam, S. A., "A novel UWB monopole antenna with tunable notched behavior using varactor diode," *IEEE Antennas. Wirel. Propag. Letters*, Vol. 13, 1243–1246, 2014.
31. Awad, N. M. and M. K. Abdelazeez, "Multislot microstrip antenna for ultra-wide band applications," *Journal of King Saud University-Engineering Sciences*, Vol. 30, No. 1, 38–45, 2018.
32. Khattak, M. I., et al., "Hexagonal printed monopole antenna with triple stop bands for UWB application," *Mehran University Research Journal of Engineering and Technology*, Vol. 38, No. 2, 335–340, 2019.
33. Li, B., Z.-H. Yan, and T.-L. Zhang, "Triple-band slot antenna with U-shaped open stub fed by asymmetric coplanar strip for WLAN/WiMAX applications," *Progress In Electromagnetics Research*, Vol. 37, 123–131, 2013.
34. Rahayu, Y. and I. R. Mustofa, "Design of 2×2 MIMO microstrip antenna rectangular patch array for 5G wireless communication network," *2017 Progress In Electromagnetics Research Symposium — Fall (PIERS — FALL)*, 2679–2683, Singapore, Nov. 19–22, 2017.
35. Khattak, M. I., et al., "Elliptical slot circular patch antenna array with dual band behaviour for future 5G mobile communication networks," *Progress In Electromagnetics Research*, Vol. 89, 133–147, 2019.